

Calculated optical properties of wurtzite InN

H. Jin, G. L. Zhao, and D. Bagayoko^{a)}

Department of Physics, Southern University and A & M College, Baton Rouge, Louisiana 70813

(Received 5 September 2006; accepted 11 December 2006; published online 14 February 2007)

We report *ab initio*, self-consistent calculations of the dielectric function of wurtzite indium nitride (*w*-InN). Our calculations employed a local density approximation (LDA) potential, a linear combination of atomic orbital basis set, and the Bagayoko-Zhao-Williams (BZW) method. Our findings agree very well with recent measurements up to photon energies of 6 eV. This excellent agreement shows the correct description, by the LDA-BZW method, of the relative separations between upper valence bands and low-lying conduction bands, in general, and corroborates our previous result of 0.88 eV for the intrinsic, fundamental band gap of *w*-InN, in particular. We also report results of simulations of the effect of high electron doping on the optical properties of InN.

© 2007 American Institute of Physics. [DOI: [10.1063/1.2435802](https://doi.org/10.1063/1.2435802)]

I. INTRODUCTION AND MOTIVATION

Wurtzite indium nitride (*w*-InN) has attracted much attention recently due not only to its numerous, potential applications but also to the recently measured band gaps, 0.7–1.0 eV, depending on temperature and particularly free carrier concentrations. Bagayoko and Franklin¹ provided an overview of two groups of experiments that reported different values of the band gap of *w*-InN. Experiments in group I, mostly before 2000, reported gaps of 1.9–2.0 eV, while the ones in group II found gaps of 0.7–1.0 eV, depending on the free carrier concentrations. Samples studied by group II, mostly grown by molecular beam epitaxy, were believed to be of much higher quality than those of group I that mostly investigated polycrystalline films. Bagayoko and Franklin¹ also discussed recent experimental reports where the band gaps of wurtzite InN are smaller than 0.7 eV, for very low free carrier concentrations (at or below 10^{18} cm⁻³), and greater than 1 eV, for very high concentrations (i.e., 10^{22} cm⁻³ or higher).

Bagayoko and Franklin obtained a theoretical band gap of 0.88 eV for *w*-InN. Their *ab initio*, zero temperature, non-relativistic, self-consistent calculations established that a band gap below 1 eV is an intrinsic property of *w*-InN, in agreement with experiments in group II. Their calculations employed density functional theory (DFT) potentials and the Bagayoko-Zhao-Williams (BZW) method that rigorously avoid a basis set and variational effect inherent to all calculations employing a linear combination of atomic orbitals (LCAOs) in variational calculations of the Rayleigh-Ritz type. The agreement between experiment and the calculated electron effective mass at the bottom of the conduction band at the Γ point indicates the correct description of the curvature of the band, at least in the vicinity of the conduction band minimum.

As in the case of the band gap, there exist two sets of experimental measurements for the optical properties of *w*-InN. Understandably, dielectric functions from the first set

show no features below 1 eV and exhibit a clear indication of an absorption edge around 2 eV,^{2–4} in accordance with the findings of the experimental group I for the band gap. In contrast, the second set^{5–10} of experiments not only shows the onset of absorption below 1 eV but also shows no features around 2 eV. A motivation for this work is to resolve the above discrepancy between two sets of experimental measurements of the dielectric functions (i.e., imaginary and real parts) of the *w*-InN. The above excellent results of the DFT-BZW approach, for the band gap and the effective mass, portend its capability in resolving this second controversy surrounding the optical properties of *w*-InN by comparing the calculated dielectric function, obtained with the *ab initio*, self-consistent, DFT-BZW bands, to experimental measurements. While the results of these calculations of the optical properties of *w*-InN are expected to show an absorption-edge-type feature around 0.8 eV, it is not *a priori* known whether or not they will also exhibit another feature around 2 eV, as suggested by the first set of measurements.

While the above discrepancy amply points to the need for this work, this need is further exacerbated by the fact that previous calculations entailed either fittings¹¹ to models of the dielectric function or a scissors-type approximation to adjust the calculated imaginary part of the dielectric function¹² or the calculated band gaps.^{13–16} The modeling work of Djurišić and Li¹¹ and the calculations of Abbar *et al.*¹³ generally agreed with the first set of measurements, i.e., with an absorption onset around 2 eV, as per the imaginary part of the dielectric function. Furthmüller *et al.*¹⁵ and Bechstedt *et al.*,¹⁶ following scissors-type adjustments to 0.81 eV of their otherwise negative, calculated band gap, reproduced dielectric functions in general agreement with the results of the second set of measurements.

II. METHOD AND COMPUTATIONAL DETAILS

We calculated the imaginary part $\varepsilon_2(\omega)$ of the complex dielectric function $\varepsilon(\omega) = \varepsilon_1(\omega) + i\varepsilon_2(\omega)$, using the Kubo-Greenwood formula.¹⁷ We utilized Kramers-Kronig relation to obtain the real part from the imaginary one. Our *ab initio*, self-consistent electronic structure computations were non-

^{a)}Author to whom correspondence should be addressed: Electronic mail: bagayoko@phys.subr.edu

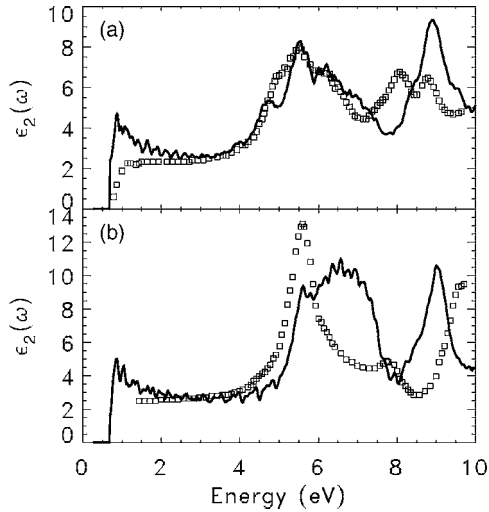


FIG. 1. The imaginary part of the dielectric function of wurtzite InN for polarizations (a) perpendicular [$\epsilon_{2xy}(\omega)$] and (b) parallel [$\epsilon_{2z}(\omega)$] to the c axis. The full lines represent our calculated results while the open squares represent experiment measurements (Ref. 6).

relativistic and they employed a local density approximation (LDA) potential,^{18,19} the linear combination of atomic orbital formalism, and the BZW method.^{1,20,21} Our program package requires, for optical property calculations, the same number of orbitals for the description of respective atomic states (i.e., s, p, d , etc.) present at the sites of the elemental species (i.e., In and N) that form the solid. Consequently, we started with *ab initio*, self-consistent calculations for In^{1+} and N^{1-} . The s, p , and d orbitals for both In^{1+} and N^{1-} were expanded by using even-tempered Gaussian functions including 20, 20, and 18 orbitals for the s, p , and d states, respectively. The Gaussian orbitals resulting from these calculations were employed in the solid computations. BZW implementation of the LCAO formalism led to an optimal basis²¹ comprising $1s2s2p3s3p3d4s4p4d5s5p$ functions for In^{1+} and $1s2s2p$ for N^{1-} . The low temperature, experimental lattice constants utilized in this work are²² $a=3.544 \text{ \AA}$, $c=5.718 \text{ \AA}$, and $u=0.3790$.

The computational error for the valence charge was about 0.000 62 for 72 electrons. The self-consistent potentials converged to a difference of 10^{-5} after about 13 iterations. Since the optical property calculations require a dense k -space mesh points, we used 4335 k -points. The calculated results for $\epsilon_2(\omega)$ and $\epsilon_1(\omega)$ were smoothed by averaging every data point with its eight adjacent neighboring points.

III. RESULTS: CALCULATED DIELECTRIC FUNCTIONS

The calculated $\epsilon_2(\omega)$ for wurtzite InN was resolved into two components, i.e., $\epsilon_{2xy}(\omega)$ and $\epsilon_{2z}(\omega)$, that are the averages of the spectra for polarizations perpendicular and parallel to the c axis, respectively. Figures 1(a) and 1(b) show $\epsilon_{2xy}(\omega)$ and $\epsilon_{2z}(\omega)$, respectively, along with recent experimental data of Goldhahn *et al.*⁶ The peak positions, shapes, and intensities of our calculated $\epsilon_2(\omega)$, in both polarization directions, are found to be in agreement with experiment up to photon energies of 6 eV, especially for the component in

the xy plane. The calculated dielectric functions exhibit the anisotropy revealed by experimental measurements. The first peaks at 0.88 eV, for $\epsilon_{2xy}(\omega)$, and at 0.85 eV, for $\epsilon_{2z}(\omega)$, indicate the onset of band edge absorption. They are measures of the direct optical band gap. Our minimum calculated band gap is 0.75 eV, which is lower than the actual theoretical minimum of 0.88 eV.¹ This difference is due to the relatively large number (i.e., 20) of Gaussian orbitals utilized to describe the s and p states on N^{1-} . Bagayoko and Franklin,¹ from the results of the atomic calculations, only needed 13 orbitals for these states on N^{1-} . As noted above, our optical property calculation software requires that we utilize the same numbers of orbitals for s and p states, respectively, for both In^{1+} and N^{1-} . The above value of 0.75 eV still falls within the range of 0.7–1.0 eV, as per the experimental group II noted above. While the above agreement of our calculated results with experiment is expected in the vicinity of the calculated band gap, the absence of features indicative of absorption, around 2 eV, is an important result. It partly settles the debate between experiments in set I and set II by establishing that high quality w -InN, in the absence of high free carrier concentrations, behave as per the findings of experiments in set II. Calculated and experimental peak positions of the imaginary part of the dielectric function, along with the possible optical interband transitions, are listed in Table I. Besides the gap structure, $\epsilon_{2xy}(\omega)$ shows six peaks which are related to critical points of the band structure (CPBSs), while $\epsilon_{2z}(\omega)$ exhibits three CPBSs. The possible optical transitions corresponding to these CPBSs, as identified from calculated results, are listed in the last two columns of Table I.

As noted above, we obtained the calculated values of the real part of the dielectric function, $\epsilon_1(\omega)$, from those of $\epsilon_2(\omega)$ by using the Kramers-Kronig relation. Figures 2(a) and 2(b) show the components of $\epsilon_1(\omega)$ in the directions perpendicular and parallel to the c axis, respectively. Again, both components of our calculated $\epsilon_1(\omega)$ agree well with experimental values up to 6 eV, in terms of peak shape, positions, and intensities. The anisotropy discussed for the imaginary part naturally carries over to the real part.

IV. DISCUSSIONS

Wu *et al.*⁹ and Ahn *et al.*⁸ have studied the effects of electron concentration on the optical properties of w -InN. Wu *et al.*⁹ reported a continuous variation of the band gap from 0.7 to 1.7 eV with increasing free carrier concentration. The latter value was for a concentration of $4.5 \times 10^{20} \text{ cm}^{-3}$. Wu *et al.*²³ found a zero temperature band gap of 0.883 eV for the intermediate concentration of $1.2 \times 10^{19} \text{ cm}^{-3}$. Inishima *et al.*²⁴ also reported a gap of 0.89 for a concentration of $5 \times 10^{19} \text{ cm}^{-3}$. The above significant Burstein-Moss shift seems to explain the disagreement between experiments in group I (with a gap around 2 eV) and those in group II (with gaps as low as 0.7 eV). For instance, the growth techniques that utilized sputtering, as was the case for several experiments in group I, are known to lead to high electron concentrations. In order to shed some light on the above explanation for relatively large band gaps, we performed a series of op-

TABLE I. Peak positions (in eV) of the imaginary part of the dielectric function $\epsilon_2(\omega)$ for InN.

Expt. ^a ϵ_{2xy}	Expt. ^a ϵ_{2z}	Calc. ^b ϵ_{2xy}	Calc. ^b ϵ_{2z}	Optical transition	Energy (eV)
4.88 ^c		4.72		$\Gamma_{4,5v}-\Gamma_{2c}$	4.62
5.35	5.38	5.54	5.54	$M_{1v}-M_{1c}$	5.64
6.05 ^c		6.16	6.62	$L_{1,2v}-L_{1,2c}$	6.09
				$L_{3,4v}-L_{1,2c}$	6.18
				$M_{2v}-M_{1c}$	6.52
				$A_{5,6v}-A_{1,2c}$	6.57
7.87	7.63	8.33 ^c		$M_{2v}-M_{2c}$	7.94
				$M_{3v}-M_{2c}$	8.49
8.60		8.85	8.95	$\Gamma_{4,5v}-\Gamma_{3c}$	8.60
				$A_{1-4v}-A_{3,4c}$	8.72
				$K_{1v}-K_{1c}$	8.87
				$K_{1v}-K_{2,3c}$	8.91
	9.44	9.51 ^c	9.90	$L_{3,4v}-L_{3,4c}$	9.34
				$M_{4v}-M_{2c}$	9.52

^aExperiment: spectroscopic ellipsometry on MBE grown InN film (Ref. 6).

^bOur calculation results.

^cShoulders.

tical property calculations for InN, with the Fermi level increased to various locations within the conduction band. We aimed to simulate the effect of the electron concentration on the optical properties of *w*-InN. By increasing the Fermi energy to conduction band, we obtained blueshifted $\epsilon_2(\omega)$ spectra. A typical calculation result is shown in Fig. 3. We depict the calculated $\epsilon_2(\omega)$ in the two polarization directions, along with the results of an experiment² in set I, in panels 3(a) and 3(b), respectively.⁶ The optical absorption edge of 1.9 eV, the previous band gap, was obtained when we increased the Fermi level from the top of valence band (TOV) to 1.85 eV above the TOV. The solid lines, in Figs. 3(a) and 3(b), represent the results of the simulation. Experiment and simulation appear to agree reasonably for photon energies up to 5 eV.

V. SUMMARY

In summary, our *ab initio*, self-consistent, DFT-BZW calculations have practically reproduced the experimental values of the dielectric function of wurtzite InN for photon energies up to 6 eV. DFT-BZW calculations are fundamentally for the description of the ground state. Hence, the disagreement between DFT-BZW results and experiments, for high photon energies, was expected. Given that the work functions of many semiconductors are around or below 6 eV, the above disagreement for high photon energies may not be a serious handicap for InN. For other semiconductors, a key issue consists of the determination of the photon energy up to which DFT-BZW and experiment agree. For photon energy above 6 eV, the CPBSs still agree fairly with experiment, as

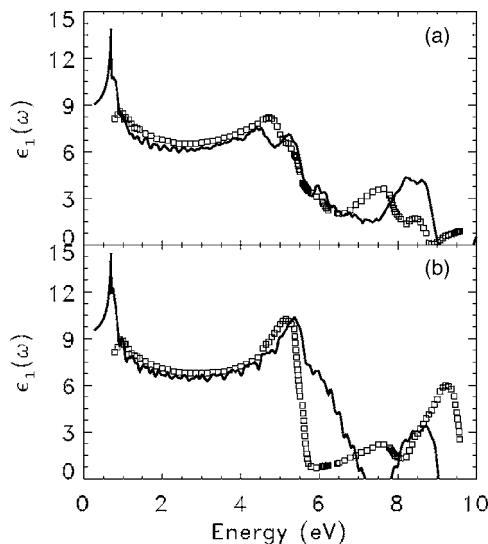


FIG. 2. The real part of the dielectric function of wurtzite InN for polarizations (a) perpendicular [$\epsilon_{1xy}(\omega)$] and (b) parallel [$\epsilon_{1z}(\omega)$] to the *c* axis. The full lines represent our calculated results while the open squares represent experiment measurements (Ref. 6).

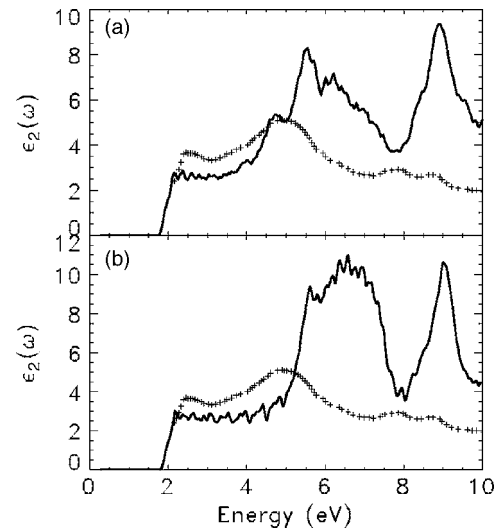


FIG. 3. The calculated imaginary part of the dielectric function for polarizations (a) perpendicular [$\epsilon_{2xy}(\omega)$] and (b) parallel [$\epsilon_{2z}(\omega)$] to the *c* axis, when the Fermi level was raised into the conduction band and was set at 1.1 eV above the bottom of the conduction. The full lines represent our calculated results while the plus symbols represent experiment measurement (Ref. 2).

per the values in Table I. The optical absorption edge of 1.9 eV was simulated by increasing the Fermi level into the conduction band. The agreement between the results of this simulation and optical properties measurements of *w*-InN samples with a large band gap (i.e., around 2 eV) appears to confirm that the increased Fermi level, as a result of high electron doping, is responsible for the large band gaps.

ACKNOWLEDGMENTS

This work was funded in part by the Department of the Navy, Office of Naval Research (ONR, Grant No. N00014-05-1-0009), NASA (Award Nos. NCC 2-1344 and NAG 5-10253), and by the National Science Foundation (Award Nos. HRD 0000272 and HRD 05-03362). The authors are indebted to L. Franklin for her help in the initial band structure calculations and to Dr. S. Hasan for his excellent technical support with the computing facilities.

¹D. Bagayoko and L. Franklin, J. Appl. Phys. **97**, 123708 (2005).

²Q. Guo, O. Kato, M. Fujisawa, and A. Yoshida, Solid State Commun. **83**, 721 (1992).

³Q. Guo, H. Ogawa, and A. Yoshida, J. Electron Spectrosc. Relat. Phenom. **79**, 9 (1996).

⁴H. F. Yang, W. Z. Shen, Z. G. Qian, Q. J. Pang, H. Ogawa, and Q. X. Guo, J. Appl. Phys. **91**, 9803 (2002).

⁵Q. Kasic, E. Valcheva, B. Monemar, H. Lu, and W. J. Schaff, Phys. Rev.

B **70**, 115217 (2004).

⁶R. Goldhahn *et al.*, Superlattices Microstruct. **36**, 591 (2004).

⁷R. Goldhahn, P. Schley, A. T. Winzer, M. Rakel, C. Cobet, N. Esser, H. Lu, and W. J. Schaff, J. Cryst. Growth **288**, 273 (2006).

⁸H. Ahn, C.-H. Shen, C.-L. Wu, and S. Gwo, Thin Solid Films **494**, 69 (2006).

⁹J. Wu *et al.*, Appl. Phys. Lett. **84**, 2805 (2004).

¹⁰W. Walukiewicz, S. X. Li, J. Wu, K. M. Yu, J. W. Ager III, E. E. Haller, H. Lu, and W. J. Schaff, J. Cryst. Growth **269**, 119 (2004).

¹¹A. B. Djurišić and E. H. Li, J. Appl. Phys. **85**, 2848 (1999).

¹²C. Persson, R. Ahuja, A. Ferreira da Silva, and B. Johansson, J. Phys.: Condens. Matter **13**, 8945 (2001).

¹³B. Abbar, B. Bouhafs, H. Aourag, G. Nouet, and P. Ruterana, Phys. Status Solidi B **228**, 457 (2001).

¹⁴N. E. Christensen and I. Gorczyca, Phys. Rev. B **50**, 4397 (1994).

¹⁵J. Furthmüller, P. H. Hahn, F. Fuchs, and F. Bechstedt, Phys. Rev. B **72**, 205106 (2005).

¹⁶F. Bechstedt, J. Furthmüller, P. H. Hahn, and F. Fuchs, J. Cryst. Growth **288**, 294 (2006).

¹⁷W. Y. Ching, J. Am. Ceram. Soc. **73**, 3153 (1990).

¹⁸D. M. Ceperley and B. J. Alder, Phys. Rev. Lett. **45**, 566 (1980).

¹⁹J. P. Perdew and A. Zunger, Phys. Rev. B **23**, 5048 (1981).

²⁰D. Bagayoko, L. Franklin, and G. L. Zhao, J. Appl. Phys. **96**, 4297 (2004).

²¹G. L. Zhao, D. Bagayoko, and T. D. Williams, Phys. Rev. B **60**, 1563 (1999); see also H. Jin, G. L. Zhao, and D. Bagayoko, *ibid.* **73**, 245214 (2006).

²²K. Osamura, S. Naka, and Y. Murakami, J. Appl. Phys. **46**, 3432 (1975).

²³J. Wu *et al.*, J. Appl. Phys. **94**, 4457 (2003).

²⁴T. Inishima, V. V. Mamutin, V. A. Vekshin, S. V. Ivanov, T. Sakon, M. Motokawa, and S. Ohoya, J. Cryst. Growth **227–228**, 481 (2002).